Supplemental material for "*Luminescent nanoparticles embedded in TiO_2 microtubes cavities for the activation of whispering-gallery-modes extending from the visible to the near infrared*"

Abbas Madani, [a, *] Libo Ma, [a] Shading Miao, [b] Matthew R. Jorgensen, [a] and Oliver G. Schmidt [a, c]

[a]*Institute for Integrative Nanosciences, IFW Dresden, Helmholtzstr. 20, 01069 Dresden, Germany*

[b]*Anhui Key Lab of Controllable Chemical Reaction & Material Chemical Engineering, School of Chemical Engineering, Hefei University of Technology, Tunxi Road. 193, 230009, Hefei, Anhui Prov. China*

[c]*Material Systems for Nanoelectronics, Chemnitz University of Technology, Reichenhainer Str. 70, 09107 Chemnitz, Germany*

1. **Luminescent NPs embedded in array of TiO_2 microtubes.** This demonstrates the feasibility of activating a large array of RUMs on single chip based on this flexible, simple, and robust technique in contrast with injection approaches.

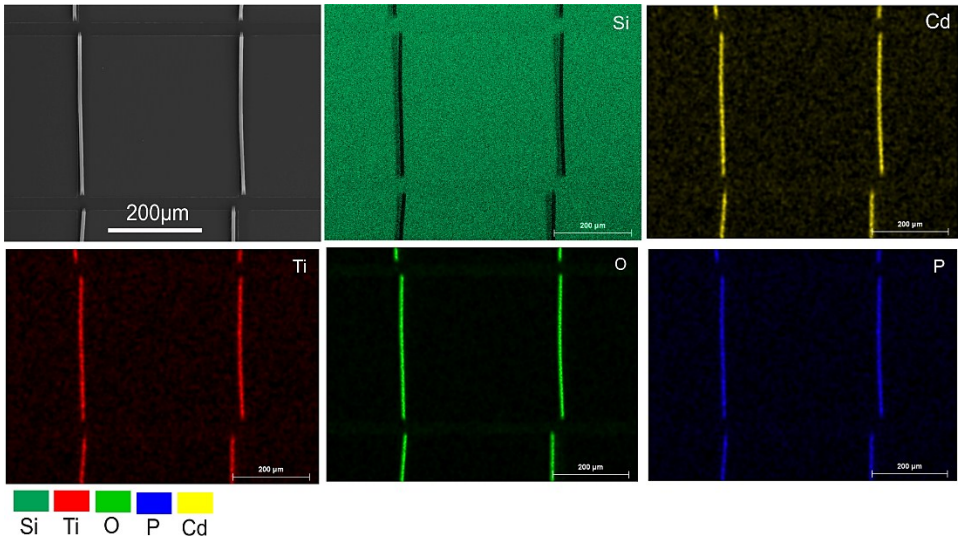

Fig. S1†. Luminescent NPs embedded in array of TiO_2 microtube walls. From top to bottom; top view SEM images of the multiple activated RUMs. The distribution of NPs was revealed by a transversal line mapping of EDX on the rolled-up microtube. The distribution of the elements Cd, P, Ti and O along the tube as well as Si in substrate were characterized.

2. **Estimation and analyzing the density of the nanoparticles** that spin coated onto the nanomembrane using ''ImageJ'' software (http://ImageJ.nih.gov/ij/). The area was shown at top panel on the left side in Fig.2 (g), where the average density of the nanoparticles is calculated to be ~ 430 per μm^2 or on the other words with an area fraction of more than ~30% into 1 μm by 1 μm area.

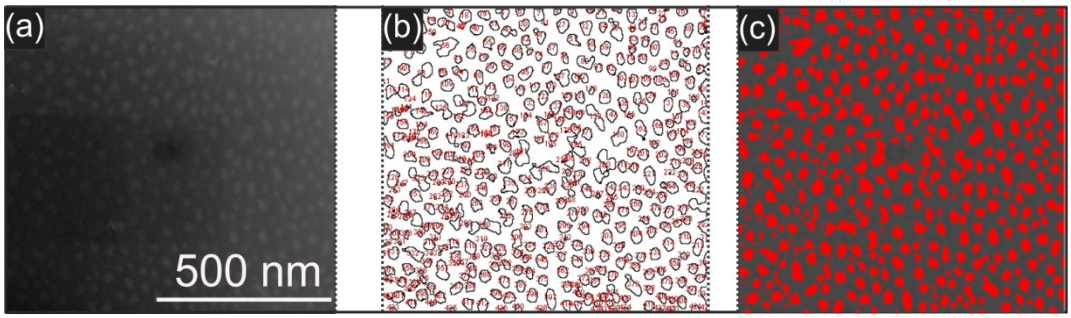

Fig. S2†. (a) Top view SEM images of assembled Cd_6P_7 NPs via spin coating of NPs onto the nanomembrane. The aggregated NPs onto the nanomembranes is imaged by ESB detector. (b) and (c) outlined and highlighted NPs region onto the 2D nanomembrane with ''ImageJ'' software, respectively. It used to count, analysis, and determine the size distribution as well as obtain the density of the NPs of NPs via spin coated onto the nanomembranes.

3. **Simulation of activated RUM with both TM and TE resonant modes and PL measured at different axial positions along the NPs-1-RUMMs in comparison with spectral profile of pure TiO_2 RU-MRRs.**

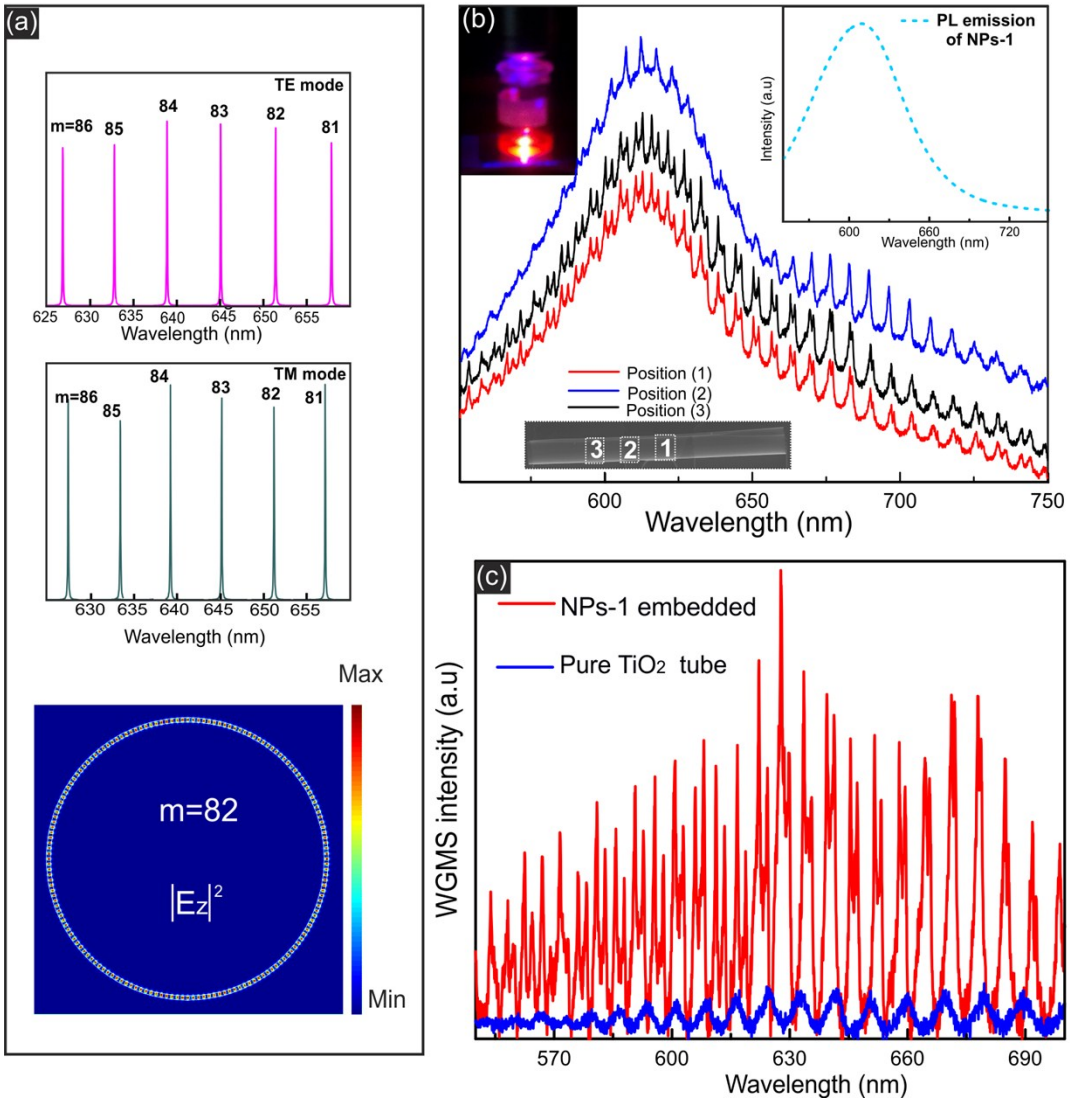

Fig. S3†. (a) 2-D simulation of activated RUM for both TM and TE resonant modes. The measured TM and TE modes are in agreement with the numerical simulations. (b) Resonant spectra of a TiO_2 microtube cavity embedded Cd_6P_7 nanoparticles (NPs-1) at three different positions on single RUM. The RUMs show multiplexing ability. A single activated TiO_2 RUM can be used as series independent ring resonators located along the tube axis. The inset on the top panel shows an optical image of the colloidal NPs-1 excited by a laser beam. The inset on the bottom panel shows SEM images of activated RUM where three measured positions are marked. The inset on the right panel shows the PL spectrum of colloidal Cd_6P_7 NPs-1. (c) Background-subtracted resonant modes spectrum of the NPs activated TiO2 microtube cavity to show the

WGMs structure more clearly for RUM with NPs-1 (red curve) and without NPs (blue curve) respectively. The WGMs intensity of TiO_2 RUM with NPs are enhanced several times in contrast to TiO_2 RUM without NPs owing to the enhanced PL emission.

4. **Resonant mode spectra and polarization mapping.**

In our preparation, the tube without embedding NPs only support TM modes (which we define as having the electric field of the resonant light parallel to the tube axis). And the NPs embedded tube supports both TM and TE (which have the electric field perpendicular to the tube axis) modes. This can be verified by polarization mappings, as shown blow. The angle equal to 0 is defined as being parallel to the tube axis.

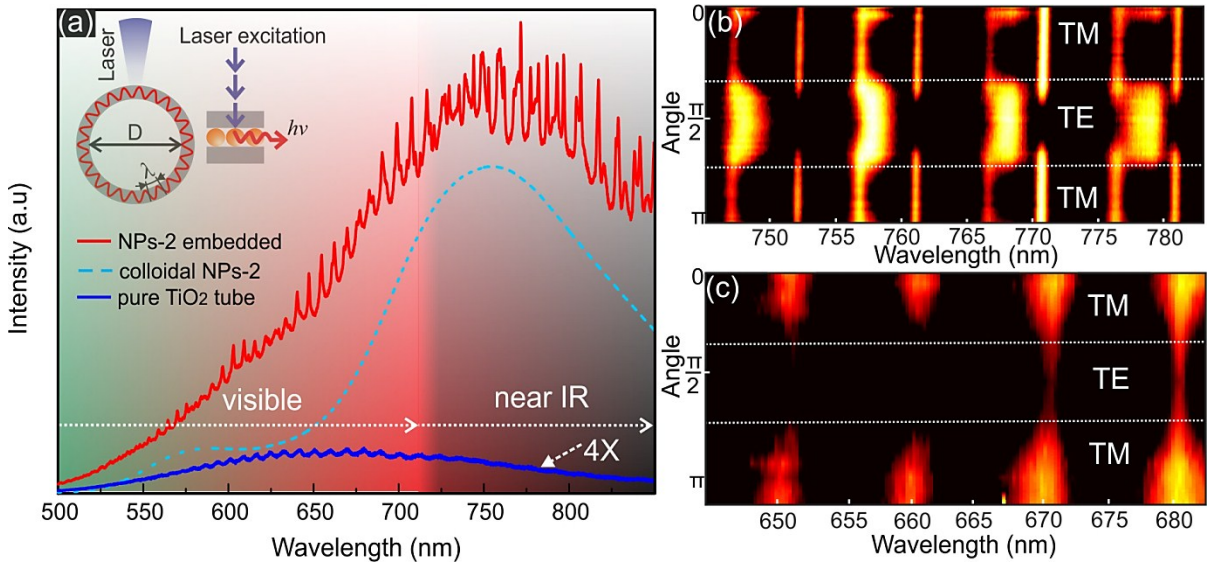

Fig. S4†. PL spectra and polarization mapping of microtubes with and without NPs-2. (a) Room temperature PL spectrum of a TiO_2 microtube cavity activated by Cd_6P_7 nanoparticles (NPs-2) (red curve), PL spectrum of a TiO_2 microtube without nanoparticles (blue curve), and PL spectrum of colloidal Cd_6P_7 NPs-2 (dashed cyan curve). (b-c) WGMs intensity as a function of polarization angle with respect to tube axis, where the both TM and TE modes for RUM with NPs-2 (top panel) and only the TM modes for RUM without NPs (bottom panel) are resolved.

5. **Enhancement of the emission intensity of WGM modes and the emission intensity of the WGMs variation of the resonant modes for both RU-MRRs with and without NPs which are in agreement with the shape of the NPs' PL spectrum**

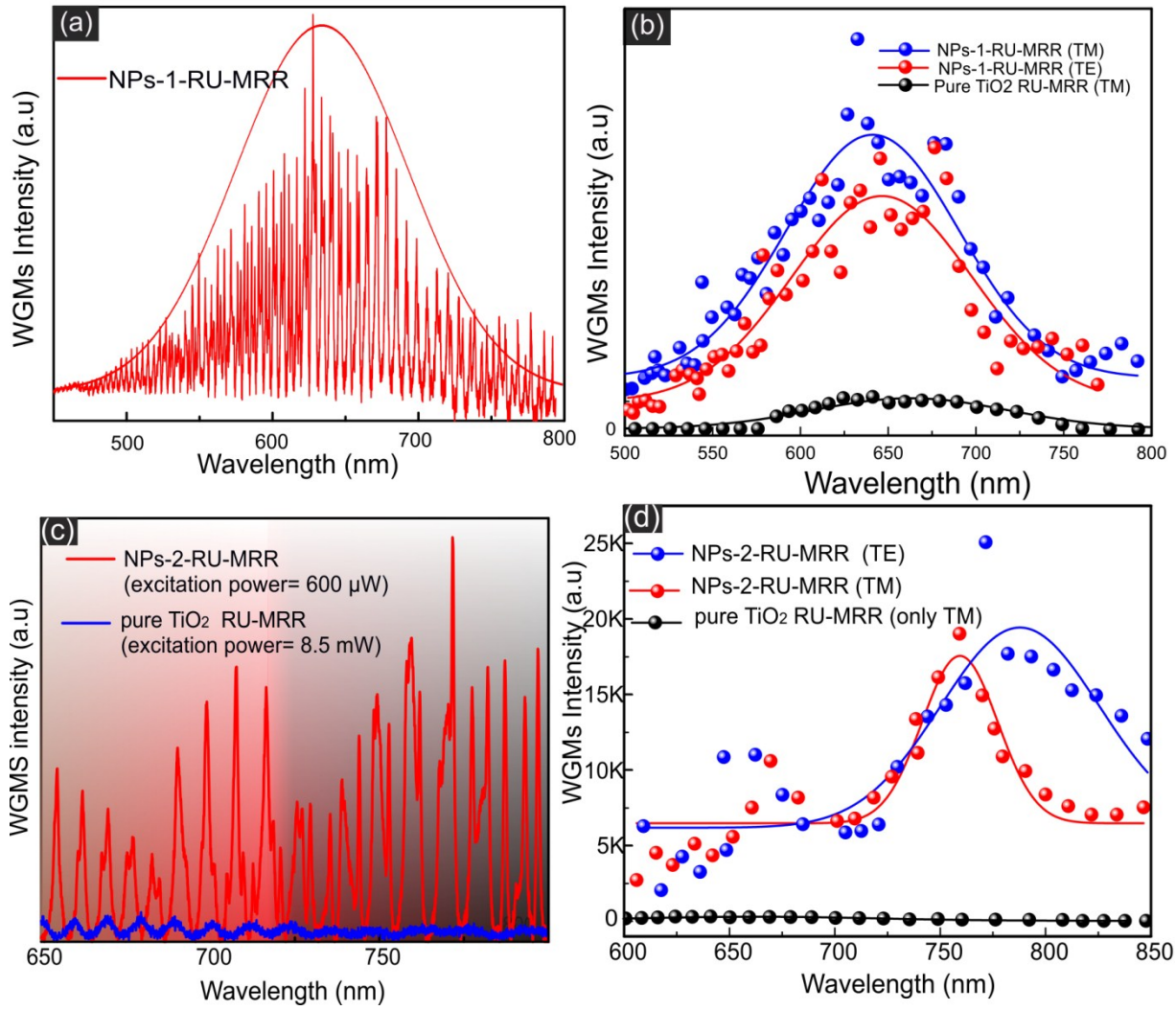

Fig. S5†. PL spectra and the variation of the emission intensity of WGMs of RU-MRRs with and without NPs. (a) and (c) Background-subtracted WGM resonant modes spectrum of the NPs activated TiO_2 microtube cavity for NPs-1-RU-MRRs and NPs-2-RU-MRRs respectively, to show the WGMs structure match the PL spectrum of colloidal Cd_6P_7 NPs in solution. (b) and (d) Spectral distribution of WGMs intensity for both TM and TE mode of both activated RU-MRRs with NPs-1 and NPs-2 respectively, in comparison with spectral profile of pure TiO_2 RU-MRRs . Note that the Pure TiO2 RU-MRRs is excited with 8.5 mW while the NPs2-RU-MRRs is exited only with 600 μW.